Covariant discretization of axis-symmetric linear optical systems

Natig M. Atakishiyev,* Shakir M. Nagiyev,† Luis Edgar Vicent,‡ and Kurt Bernardo Wolf

Centro de Ciencias Físicas, Universidad Nacional Autónoma de México, Apartado Postal 48-3, 62251 Cuernavaca, Morelos, Mexico

Received February 25, 2000; revised manuscript received July 21, 2000; accepted July 25, 2000

We propose a discretization strategy for systems with axial symmetry. This strategy replaces the continuous position coordinates by a discrete set of sensor points, on which the discrete wave fields transform covariantly with the group of 2×2 symplectic matrices. We examine polar arrays of sensors (i.e., numbered by radius and angle) and find the complete, orthonormal sets of discrete-waveguide Meixner functions; when the sensors come closer together, these tend to the Laguerre eigenmodes of the continuous waveguide. In particular, the fractional Hankel transforms are discretized in order to define the fractional Hankel–Meixner transforms and similarly for all axis-symmetric linear optical maps. Coherent states appear in the discrete cylindrical waveguide. Covariant discretization leads to the same Wigner phase-space function for both the discrete and the continuum cases. This reinforces a Lie-theoretical model for the phase space of discrete systems. © 2000 Optical Society of America [S0740-3232(00)01512-X]

OCIS codes: 000.3860, 070.4560, 200.4560, 350.6980.

1. INTRODUCTION

We propose a strategy to discretize three-dimensional (3D) paraxial optical systems: We match the transformations of the wave fields on a continuous screen, using the same group of transformations of a wave matrix defined on a two-dimensional (2D) array of sensor points. This covariant discretization must, moreover, agree with the requirement that, when the sensors come closer together (in a well-defined limit), the matrices of the discrete systems will tend to the canonical integral transform kernel of the continuous system.

The transformations that we consider are those produced by paraxial optical systems that are symmetric under rotations about the optical axis, i.e., linear, symplectic transformations of phase space that belong to the group $\mathrm{Sp}(2, \Re)$. On continuous wave fields this group is represented by the radial canonical integral transforms studied within the context of 2D quantum oscillators by Moshinsky *et al.*[1] in 1972. The same group $\mathrm{Sp}(2, \Re)$ has infinite, lower-bound matrix representations that have been studied by Bargmann[2] and many others since 1947. The matrix and the integral kernel are but two distinct subgroup-reduced representations of the same linear optical system. In this matrix representation the row index has the interpretation of the discrete radial position coordinate of a circle of sensors on the screen. Lastly, the discretization of the angular coordinate proceeds through the well-known restriction from Fourier series on the circle to finite Fourier series on an equally spaced subset of points.

This paper is aimed at the fundamental problem of discretization, which is solved in an $\mathrm{Sp}(2, \Re)$-covariant way. In a previous paper,[3] using SU(2) with a method not coincident with the present one, we discretized 2D paraxial waveguide systems that have 1D screens. Oscillator functions and coherent states of the continuum were put into correspondence with discrete and finite counterparts involving Kravchuk functions.[4,5] When we started tackling the 3D case on 2D screens it was evident[3] that a Cartesian separation of coordinates yields simply two independent 1D discrete systems, on a Cartesian sensor array such as that shown in Fig. 1(a). But it was also clear that axially symmetric optical systems could be poorly represented in the Cartesian scheme. An obvious choice would be to place the sensors in a star pattern, such as that shown in Fig. 1(b), with the same number of equidistant sensors on a series of equally spaced concentric circles. The fast finite Fourier transform could be performed on each circle, and a (more difficult) discrete Hankel-type transform could be performed among the radii (in acoustics, the Hankel part has been studied numerically in Ref. 6). One problem with this simple star sampling of functions on the plane is that it is not of homogeneous density; another problem is that it is difficult to say how a simple linear axis-symmetric optical system will transform the values of a given set of wave-field data without going through ill-defined continua. Thus we set as our objective to discretize the plane in polar coordinates, using Lie algebras with a new optical interpretation. As we shall see, we solve both problems of the star array with a covariant discretization of the plane into sensor arrays such as that shown in Fig. 1(c).

In Section 2 we assemble known facts about radial canonical integral transforms, which represent the action of axis-symmetric linear optical systems on the (generally asymmetric) input wave field, in polar coordinates. In particular, the Fourier transform decomposes into a Fourier series of Hankel transforms of discrete order m related to the Petzval invariant (angular momentum) of the partial wave field. Here the radial position and angle coordinates are continuous, and the waveguide eigenfunctions involve Laguerre functions of the square radius,

0740-3232/2000/122301-14$15.00

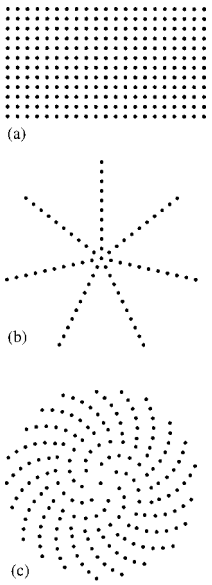

Fig. 1. Two-dimensional arrays of sensors admitting separation in (a) Cartesian and (b), (c), polar coordinates, further characterized in the text. Arrays (a) and (c) exhibit a homogeneous density of sensors on the plane. The arrays considered in this paper are of type (c).

times angle-dependent phases. Section 3 lists the differential operators that generate free and waveguide evolution as well as Gaussian lens action. Among the generators we identify the square position and momentum operators, as well as the waveguide Hamiltonian, whose eigenvalues provide the continuous and the discrete coordinates, respectively. Section 4 recalls results that were obtained on the same group Sp(2, $\Re$) but that were represented by matrices that Bargmann called[2] the discrete series of representations, D_k^+; we find that $k = (1/2)(1 + |m|)$. The generators of discrete optical systems are written as difference operators. The radial part of the normal modes of discrete harmonic waveguides are the Meixner functions previously studied in Ref. 7.

The radial part of 2D discrete systems can have a centrifugal or Petzval core and a waveguide width (harmonic potential strength); these two values determine the two parameters of the Meixner functions. In Section 5 we define the *Meixner* transform as scaling to the continuum limit. In particular, in Section 6 we study the fractional Hankel–Meixner transform that discretizes the fractional Hankel integral transforms. In Section 7 we put these results back into the problem of the 2D polar-separated array of sensors. Covariant discretization correctly reproduces the coherent states that spiral along a waveguide, as shown in Section 8, and the linear canonical transformations given in Section 9. In Section 10 we reflect on the meaning of the optical phase space and on the ways to represent discrete beams through their Wigner functions.

The subject of separation of (continuous) variables has a rich literature.[8] Separation of discrete coordinates could be an interesting subject in which group-theoretical considerations will play their role again. The limited aim of this paper, however, is to apply classical representation theory of the group of 2×2 matrices to discretize the plane in polar coordinates and thus model discrete (axis-symmetric, paraxial) optical systems. In concluding (Section 11), we recapitulate the results and offer some avenues for application of the theory of 2×2 matrices.

2. RADIAL CANONICAL INTEGRAL TRANSFORMS

Our starting point is the group of linear symplectic (canonical) transformations in two coordinates of position and their canonically conjugate momenta, Sp(4, $\Re$). This group has ten parameters; it can be realized through paraxial optical systems built only of astigmatic lenses and free spaces.[9] One subgroup reduction,

$$\mathrm{Sp}(4,\Re) \supset \mathrm{Sp}(2,\Re)_x \otimes \mathrm{Sp}(2,\Re)_y, \tag{1}$$

occurs when all astigmatic lenses have aligned principal axes, and it conveniently simplifies considerations to two independent 2D optical systems along the x and the y axes. (With a subindex we indicate the coordinate on which the group acts, to avoid confusion.) The subgroup reduction that we shall develop here is adapted to radial and angular coordinates on the screens; it is

$$\mathrm{Sp}(4,\Re) \supset \mathrm{SO}(2)_\theta \otimes \mathrm{Sp}(2,\Re)_r, \tag{2}$$

where $\mathrm{SO}(2)_\theta$ is the 1D group of rotations of the x–y plane by $\theta \in \mathcal{S}^1$ (the circle) and $\mathrm{Sp}(2,\Re)_r$ is the symplectic group in the radial coordinate $r \in \Re_0^+ = [0, \infty)$. The latter group includes the Hankel fractional transforms and quadratic phase factors produced by axially symmetric paraxial optical systems.

The wave fields $\psi(\mathbf{q})$ on the screen $\mathbf{q} \in \Re^2$ need not be axially symmetric, of course. Rather, when we express the argument in polar coordinates,

$$q_x = r\cos\theta, \qquad q_y = r\sin\theta, \qquad r \in \Re_0^+, \qquad \theta \in \mathcal{S}^1, \tag{3}$$

we can expand $\psi(\mathbf{q}) = \psi(r, \theta)$ into Fourier series in θ as

$$\sqrt{r}\psi(r,\theta) = \frac{1}{\sqrt{2\pi}} \sum_{m=-\infty}^{\infty} \psi_m^{\mathrm{H}}(r) e^{im\theta},$$

$$\psi_m^{\mathrm{H}}(r) = \frac{1}{\sqrt{2\pi}} \int_{\mathcal{S}^1} \mathrm{d}\theta \sqrt{r}\psi(r,\theta) e^{-im\theta}. \tag{4}$$

The factor $\sqrt{r}$ is placed so that square-integrable wave fields (over $\mathbf{q} \in \Re^2$ with measure $\mathrm{d}q_x\mathrm{d}q_y = r\mathrm{d}r\mathrm{d}\theta$) map to sequences of square-integrable functions $\psi_m^{\mathrm{H}}(r)$, $m \in \mathcal{Z}$ (the integers), each belonging to a Hilbert space $\mathcal{L}^2(\Re_0^+)$ of square-integrable functions

$$(\phi, \psi)_{\mathcal{L}^2} = \int_{\Re_0^+} \mathrm{d}r\, \phi(r)^* \psi(r) \tag{5}$$

with respect to the measure $\mathrm{d}r$.

As a prime example we consider the case of the 2D axis-symmetric Fourier transform. This is an operator that maps $\mathcal{L}^2(\Re^2)$ on itself unitarily; it is represented by the well-known integral transform[10,11]

$$(\mathcal{F}\colon \psi)(\mathbf{q}) = \frac{1}{2\pi} \int_{\Re^2} \mathrm{d}\mathbf{q}'\, \exp(-i\mathbf{q}\cdot\mathbf{q}')\psi(\mathbf{q}'). \tag{6}$$

We express the wave fields and the integral kernel of Eq. (6) in polar coordinates (3) by means of the generating function

$$\exp(i\mathbf{q}\cdot\mathbf{q}') = \exp[irr'\cos(\theta-\theta')] = \sum_{m\in\mathcal{Z}} i^m J_m(rr')\exp[im(\theta-\theta')], \quad (7)$$

where $J_m(x)$ are the Bessel functions of the first kind. Then the Fourier transform decomposes as

$$(\mathcal{F}:\psi)(r,\theta) = \sum_{m\in\mathcal{Z}} \frac{e^{im\theta}}{\sqrt{2\pi r}}(-i)^m(\mathcal{H}_m : \psi_m^{\mathrm{H}})(r), \quad (8)$$

namely, into the direct sum of Hankel transforms of integer order m—called helicity here—that act on the corresponding partial wave fields $\phi(r) = \psi_m^{\mathrm{H}}(r)$:

$$(\mathcal{H}_m : \phi)(r) = i^m\left(\frac{r}{2\pi}\right)^{1/2}\int_{\mathcal{S}^1} \mathrm{d}\theta e^{-im\theta}(\mathcal{F}:\phi)(r,\theta) = \int_{\mathfrak{R}_0^+}\mathrm{d}r' H_m^1(r,r')\phi(r'), \quad (9)$$

$$H_m^1(r,r') = \sqrt{rr'}J_m(rr'), \quad (10)$$

where we recall the property $J_{-m}(x) = (-1)^m J_m(x) = J_m(-x)$. Finally, we can invert the 2D Fourier transform (6) to find the partial-m wave fields, first integrating over circles on the screen and then performing the inverse Hankel transform of helicity m among the circles. The Fourier transform thus unfolds the subgroup reduction (2) into a Fourier series of Hankel transforms and separates the screen into polar coordinates.[8]

Axis-symmetric optical systems are commonly represented (in geometric and Fourier optics) by 4×4 symplectic matrices with 2×2 blocks that are multiples a, b, c, d of the 2×2 unit matrix, and $ad-bc=1$. They also have the 2D canonical integral transform representation

$$[\mathcal{C}(\mathbf{M}) : \psi](\mathbf{q}) = \int_{\mathfrak{R}^2}\mathrm{d}\mathbf{q}' C_{\mathrm{M}}(\mathbf{q},\mathbf{q}')\psi(\mathbf{q}'), \qquad \mathbf{M} = \begin{bmatrix} a & b \\ c & d\end{bmatrix}, \quad (11)$$

$$C_{\mathrm{M}}(\mathbf{q},\mathbf{q}') = \frac{1}{2\pi i b}\exp i\left(\frac{d}{2b}|\mathbf{q}|^2 - \frac{\mathbf{q}'\cdot\mathbf{q}}{b} + \frac{a}{2b}|\mathbf{q}'|^2\right). \quad (12)$$

In particular, for $\mathbf{H} = \left[\begin{smallmatrix} 0 & 1 \\ -1 & 0\end{smallmatrix}\right]$, we have $\mathcal{C}(\mathbf{H}) = -i\mathcal{F}$. Performing steps (6)–(10), we find the radial $\mathrm{Sp}(2,\mathfrak{R})_r$ transform [1,12] of helicity $m\in\mathcal{Z}$ by restricting Eq. (12) to the subspaces of partial wave fields [Ref. 13, Eqs. (25)]:

$$[\mathcal{C}(\mathbf{M}) : \psi](r,\theta) = \sum_{m\in\mathcal{Z}}\frac{e^{im\theta}}{\sqrt{2\pi r}}[\mathcal{C}(\mathbf{M})|_m : \psi_m^{\mathrm{H}}](r), \quad (13)$$

$$[\mathcal{C}(\mathbf{M})|_m : \phi](r) = \int_{\mathfrak{R}_0^+}\mathrm{d}r' C_{\mathrm{M}}^{|m|}(r,r')\phi(r'), \quad (14)$$

$$C_{\mathrm{M}}^{|m|}(r,r') = \frac{1}{i^{|m|+1}b}\sqrt{rr'}\exp\left(\frac{id}{2b}r^2\right)J_{|m|}\left(\frac{rr'}{b}\right)\times\exp\left(\frac{ia}{2b}r'^2\right). \quad (15)$$

When $c=0$ and $a=d=1$, Eqs. (11)–(15) yield the 2D Fresnel transform of free flight by the optical distance b. When $b\to 0$ the canonical integral transform becomes a geometric transform (which reproduces images) with a limit in the mean given by

$$\left[\mathcal{C}\begin{bmatrix} a & 0 \\ c & a^{-1}\end{bmatrix}\Big|_m : \phi\right](r) = \frac{(\mathrm{sign}\,a)^m}{\sqrt{|a|}}\exp\left(\frac{ic}{2a}r^2\right)\phi\left(\frac{r}{|a|}\right). \quad (16)$$

These elements include Gaussian thin lenses for $a=d=1$ and pure magnifiers by a factor of $a=d^{-1}$ for $c=0$.

The optical elements concatenate as their 2×2 matrices multiply: From $\mathcal{C}(\mathbf{M}_1)\times\mathcal{C}(\mathbf{M}_2) = \mathcal{C}(\mathbf{M}_1\mathbf{M}_2)$, when the operator domain is restricted to the partial wave field m, the radial canonical transform kernels (15) will satisfy

$$\int_{\mathfrak{R}_0^+}\mathrm{d}r' C_{\mathrm{M}_1}^{|m|}(r,r')C_{\mathrm{M}_2}^{|m|}(r',r'') = C_{\mathrm{M}_1\mathrm{M}_2}^{|m|}(r,r''). \quad (17)$$

The unit is $\mathcal{C}(\mathbf{1}) = 1$, but the second commuting element is different in each subspace: $\mathcal{C}(-\mathbf{1})|_m = (-1)^m 1$. Associativity holds, and the inverse is $\mathcal{C}(\mathbf{M}^{-1}) = [\mathcal{C}(\mathbf{M})]^{-1}$. This group of operators is unitarily represented in $\mathcal{L}^2(\mathfrak{R}_0^+)$, i.e., $C_{\mathrm{M}^{-1}}^{|m|}(r,r') = C_{\mathrm{M}}^{|m|}(r',r)^*$. Moreover, the representation labeled by m is irreducible; i.e., it cannot be further decomposed into invariant subspaces. It is important to point out that the (sometimes problematic) metaplectic sign of $\mathrm{Sp}(4,\mathfrak{R})$ does not enter here because in axis-symmetric optical systems the two metaplectic signs in the orthogonal x and y directions exactly cancel.

Again for the Fourier transform, $\mathbf{H} = \left[\begin{smallmatrix} 0 & 1 \\ -1 & 0\end{smallmatrix}\right]$, and we have $C_{\mathrm{H}}^{|m|} = (-i)^{|m|+1}H_m^1(r,r')$, as given in Eq. (10). This observation leads us to define the Hankel transforms of fractional power α (counted modulo 4) and helicity (order) m by

$$\mathcal{H}_m^\alpha = \exp[i\tfrac{1}{2}\pi(|m|+1)\alpha]\mathcal{C}(\mathbf{H}^\alpha)|_m, \qquad \mathbf{H}^\alpha = \begin{bmatrix} \cos\frac{1}{2}\pi\alpha & \sin\frac{1}{2}\pi\alpha \\ -\sin\frac{1}{2}\pi\alpha & \cos\frac{1}{2}\pi\alpha\end{bmatrix}, \quad (18)$$

where we call $\mathbf{H}^\alpha$ the fractional Hankel matrix. The phase is chosen to match the classical form, as was done in Ref. 3 for the fractional Fourier transform. The integral kernel of the fractional Hankel transform is thus

$$H_m^\alpha(r,r') = \frac{1}{\sin(\pi/2)\alpha}\sqrt{rr'}\exp\left[i\frac{1}{2}(r^2+r'^2)\times\cot\frac{\pi}{2}\alpha\right]J_m\left[\frac{rr'}{\sin(\pi/2)\alpha}\right]. \quad (19)$$

3. GENERATORS OF OPTICAL SYSTEMS

The circle of fractional Hankel transforms is a continuous one-parameter Lie group: $\mathcal{H}_m^{\alpha_1}\mathcal{H}_m^{\alpha_2} = \mathcal{H}_m^{\alpha_1+\alpha_2}$, with powers α modulo 4. Considering α's close to zero (the identity element), we can write the fractional Hankel transforms (18) as hyperdifferential operators,

$$\mathcal{H}_m^{\alpha} = \exp[i\tfrac{1}{2}\pi(|m|+1)\alpha]\exp(-i\tfrac{1}{2}\pi\alpha\hat{H}_m), \quad (20)$$

where we find the generator of the subgroup on $\phi(r) = \psi_m^{\mathrm{H}}(r)$ through

$$\begin{aligned}\lim_{\alpha\to 0}\frac{2i}{\pi\alpha}\{[\mathcal{C}(\mathbf{H}^{\alpha})|_m - 1] : \phi\}(r) &= \hat{H}_m\phi(r)\\ &= \frac{1}{2}\left[-\frac{\partial^2}{\partial r^2} + \frac{m^2-(1/4)}{r^2} + r^2\right]\phi(r). \end{aligned} \quad (21)$$

The operator $\hat{H}_m$ in Eq. (21) is the evolution operator for displacements along a waveguide of wave fields with helicity m and is also the Hamiltonian of a 1D quantum harmonic oscillator (of unit mass and spring constant) plus a centrifugal potential core c/r^2 of strength $c = m^2-(1/4)$ [i.e., circular oscillator in polar coordinates (see Ref. 14)]. Although in the waveguide model only integer values of m are of interest, continuous c appears in the quantum model. In particular, the zero-helicity optical wave fields $m = 0$ correspond to quantum wave functions of an oscillator with a weakly centripetal core $c = -(1/4)$. [Indeed, $-(1/4) \leqslant c \leqslant (3/4)$ is known as the exceptional interval of Sp(2, $\Re$) because it requires a rather delicate functional analysis of self-adjoint extensions of this second-order differential operator that we will not reproduce here; it is detailed in Ref. 15]. In the Hilbert space $\mathcal{L}^2(\Re_0^+)$ the spectrum (i.e., the set of eigenvalues) of $\hat{H}_m$ in Eqs. (21) is well known to be equally spaced and bounded from below:

$$\hat{H}_m\Psi_{m,n}^{\mathrm{H}}(r) = E_n^{|m|}\Psi_{m,n}^{\mathrm{H}}(r),$$
$$E_n^{|m|} = 2n + |m| + 1, \qquad n \in \mathcal{Z}_0^+ = \{0, 1, 2, \ldots\}, \quad (22)$$

with eigenfunctions of mode number n that are the Laguerre functions of r^2, and which depend only on the absolute value of the helicity,

$$\Psi_{m,n}^{\mathrm{H}}(r) = \left[\frac{2n!}{(|m|+n)!}\right]^{1/2} e^{-r^2/2}r^{|m|+1/2}L_n^{|m|}(r^2). \quad (23)$$

In Ref. 16 Ojeda-Castañeda and Noyola-Iglesias studied the wave functions (23) as nondiffracting beams in a cylindrical harmonic graded-index waveguide. [Notice that in Ref. 7 a sign $(-1)^n$ was used in the definition of Eq. (23) because there it was important to agree with the standard radial hydrogenic wave functions of Landau and Lifshitz.[17]] Because of Eq. (20), these functions self-reproduce under the fractional Hankel transform

$$\begin{aligned}(\mathcal{H}_m^{\alpha} : \Psi_{m,n}^{\mathrm{H}})(r) &= \exp[i\tfrac{1}{2}\pi(|m|+1-E_n^{|m|})\alpha]\Psi_{m,n}^{\mathrm{H}}(r)\\ &= \exp(-i\pi n\alpha)\Psi_{m,n}^{\mathrm{H}}(r). \end{aligned} \quad (24)$$

The same limiting procedure, which led us to find the generator $\hat{H}_m$ in Eq. (21) of the Hankel transform subgroup (18), can be applied to other subgroups of $\mathrm{Sp}(2,\Re)_r$. We establish uniform nomenclature through the following relations:

$$\exp[i\theta\hat{J}_0^{(m)}] = \mathcal{C}\begin{bmatrix}\cos(\theta/2) & -\sin(\theta/2)\\ \sin(\theta/2) & \cos(\theta/2)\end{bmatrix}\Bigg|_m$$
$$\Rightarrow \hat{J}_0^{(m)} = \frac{1}{4}\left[-\frac{\partial^2}{\partial r^2} + \frac{m^2-(1/4)}{r^2} + r^2\right], \quad (25)$$

$$\exp[i\eta\hat{J}_1^{(m)}] = \mathcal{C}\begin{bmatrix}\cosh(\eta/2) & -\sinh(\eta/2)\\ -\sinh(\eta/2) & \cosh(\eta/2)\end{bmatrix}\Bigg|_m$$
$$\Rightarrow \hat{J}_1^{(m)} = \frac{1}{4}\left[-\frac{\partial^2}{\partial r^2} + \frac{m^2-(1/4)}{r^2} - r^2\right], \quad (26)$$

$$\exp[i\zeta\hat{J}_2^{(m)}] = \mathcal{C}\begin{bmatrix}e^{-\zeta/2} & 0\\ 0 & e^{\zeta/2}\end{bmatrix}\Bigg|_m$$
$$\Rightarrow \hat{J}_2^{(m)} = -\frac{i}{2}\left(r\frac{\partial}{\partial r} + \frac{1}{2}\right), \quad (27)$$

and we also note the following linear combinations:

$$\exp[ib\hat{J}_+^{(m)}] = \mathcal{C}\begin{bmatrix}1 & -b\\ 0 & 1\end{bmatrix}\Bigg|_m$$
$$\Rightarrow \hat{J}_+^{(m)} = \hat{J}_0^{(m)} + \hat{J}_1^{(m)} = \frac{1}{2}\left[-\frac{\partial^2}{\partial r^2} + \frac{m^2-(1/4)}{r^2}\right], \quad (28)$$

$$\exp[ic\hat{J}_-^{(m)}] = \mathcal{C}\begin{bmatrix}1 & 0\\ c & 1\end{bmatrix}\Bigg|_m \Rightarrow \hat{J}_-^{(m)} = \hat{J}_0^{(m)} - \hat{J}_1^{(m)} = \frac{1}{2}r^2. \quad (29)$$

Under commutation these operators are a vector basis for the Lie algebra $\mathrm{sp}(2,\Re)_r$:

$$[\hat{J}_0^{(m)}, \hat{J}_1^{(m)}] = i\hat{J}_2^{(m)}, \qquad [\hat{J}_1^{(m)}, \hat{J}_2^{(m)}] = -i\hat{J}_0^{(m)},$$
$$[\hat{J}_2^{(m)}, \hat{J}_0^{(m)}] = i\hat{J}_1^{(m)}. \quad (30)$$

The quadratic invariant (Casimir) operator is essentially the square helicity invariant (Petzval) of the wave field:

$$\hat{J}^{(m)2} = \hat{J}_1^{(m)2} + \hat{J}_2^{(m)2} - \hat{J}_0^{(m)2} = \tfrac{1}{2}(1-m^2) \leqslant \tfrac{1}{2}. \quad (31)$$

The generators (25)–(29) will be the continuum limit of the covariant discretization scheme of this paper. We especially point out two operators that will play an important role in what follows: $\hat{J}_0^{(m)} = (1/2)\hat{H}_m$ (cf. the waveguide evolution Hamiltonian), which has a discrete, lower-bound spectrum $n + (1/2)(|m|+1)$, $n \in \mathcal{Z}_0^+$; and $\hat{J}_-^{(m)}$, which is the operator that is diagonal in the canoni-

cal transform representation and has a continuous spectrum $\rho = (1/2)r^2$, $r \in \Re_0^+$, and which we henceforth identify with the one-half-square radius operator of position on the screen. Its integrated group action on the wave fields is that of a thin lens that impresses a Gaussian radial phase factor $\exp(i\gamma r^2)$. There is also the Fourier transform of $\hat{J}_-$, namely, the free centrifugal Hamiltonian $\hat{J}_+^{(m)}$ in relation (28) for wave fields of helicity $|m|$; its integral kernel (15) is the radial part of the 2D Fresnel transform. Finally, among the generators listed above, there are also the (one-half) radial repulsive waveguide Hamiltonian in relation (26), and the scaling generator in relation (27); their common spectrum is $\lambda \in \Re$.

4. DISCRETE REPRESENTATIONS OF Sp(2, $\Re$)

The group of 2×2 matrices, representing axis-symmetric optical systems, has a rich manifold of representations. Following Bargmann's traditional nomenclature,[2] we shall refer to the discrete-series lower-bound representations D_+^k, which are unique in that J_0 has a lower bound on its (energy) eigenvalues. [The designation "discrete" for D_k^+ is historical but is rather inconvenient here, because we shall also work with discrete (but distinct, i.e., denumerable) eigenbases; moreover, we may allow for continuous values of m.] There are also the continuous representation series that are obtained by the separation of 2D canonical transforms in hyperbolic coordinates;[18] these will not further concern us here.

The D_+^k representations in a continuous basis are the integral kernels (19) of Section 3; here we write them in a discrete basis, quoting classical results.[2] Henceforth we reserve the letters m for helicity and k for the Bargmann label, which in this optical waveguide model are related by

$$|m| = 2k - 1, \qquad k = \tfrac{1}{2}(|m| + 1) \in \{\tfrac{1}{2}, 1, \tfrac{3}{2}, 2, \ldots\}. \tag{32}$$

Using the Laguerre function basis (23) and the inner product (5), we establish the following representation matrices with rows and columns labeled by $n, n' \in \mathcal{Z}_0^+$ [cf. Ref. 13, Eq. (3.22)]:

$$D^k_{n,n'}(\mathbf{M}) = \left(\Psi^{\mathrm{H}}_{m,n}, \mathcal{C}\begin{bmatrix} a & b \\ c & d \end{bmatrix} : \Psi^{\mathrm{H}}_{m,n'} \right)_{\mathcal{L}^2} \tag{33}$$

$$= \frac{[(d-a) - i(b+c)]^n [(a-d) - i(b+c)]^{n'} [(a+d) + i(b-c)]^{-2k-n-n'}}{[n!n'!\Gamma(2k+n)\Gamma(2k+n')]^{1/2}} 2^{2k}\Gamma(2k+n+n') \times F\left[\begin{matrix} -n, & -n' \\ 1-2k-n-n' \end{matrix}; \ \frac{a^2+b^2+c^2+d^2+2}{a^2+b^2+c^2+d^2-2} \right], \tag{34}$$

where $F[\begin{smallmatrix} u, & v \\ w \end{smallmatrix}; z]$ is the Gauss hypergeometric function, which in this case is a polynomial in z of degree $\min(n, n')$. In Appendix A we use the linear relation among hypergeometric functions of z, $1 - z$, and $1/z$ to show that the representation of the Hankel matrix (18) for $\theta = (1/2)\pi\alpha$ is

$$D^k_{n,n'}\begin{bmatrix} \cos\theta & \sin\theta \\ -\sin\theta & \cos\theta \end{bmatrix} = \exp[-2i(k+n)\theta]\delta_{n,n'}. \tag{35}$$

While the axis-symmetric optical system $\mathbf{M}$ acts on (the mth partial) continuous wave fields $\psi(r)$ through the radial canonical integral transform [Eqs. (14) and (15)] of helicity m, it will act in D_k^+ on a discrete wave field $\psi(n)$, $n \in \mathcal{Z}_0^+$, through

$$[\mathcal{C}(\mathbf{M})|^k : \psi](n) = \sum_{n' \in \mathcal{Z}_0^+} D^k_{n,n'}(\mathbf{M})\psi(n'), \tag{36}$$

where $|^k = |_m$ and the D-matrix elements are as given in Eqs. (33), (34), and (A1) (Appendix A). The fundamental property of the matrices is to represent the group Sp(2, $\Re$), i.e.,

$$\sum_{n' \in \mathcal{Z}_0^+} D^k_{n,n'}(\mathbf{M}_1) D^k_{n',n''}(\mathbf{M}_2) = D^k_{n,n''}(\mathbf{M}_1\mathbf{M}_2). \tag{37}$$

In these representations $D^k_{n,n'}(\pm\mathbf{1}) = (\pm 1)^{2k}\delta_{n,n'}$ [Eq. (35) for $\theta = \pi$]; hence the half-integer D_k^+'s (m odd) correspond to faithful representations of Sp(2, $\Re$), while the integer D_k^+'s (m even) correspond to faithful representations of SO(2, 1), the original group studied by Bargmann. The Hilbert space here is $\ell^2(\mathcal{Z}_0^+)$, the space of square-summable sequences under the natural inner product

$$(\phi^{\mathrm{H}}, \psi^{\mathrm{H}})_{\ell^2} = \sum_{n \in \mathcal{Z}_0^+} \phi^{\mathrm{H}*}_n \psi^{\mathrm{H}}_n. \tag{38}$$

The matrix kernels are unitary and irreducible.[2]

In the continuum the generators of the 2D symplectic Lie algebra sp(2, $\Re$), J_σ, $\sigma = 0, 1, 2, \pm$, were realized by first- and second-order differential operators (25)–(29); the hat (caret) of $\hat{J}_\sigma^{(m)}$ is meant to remind us of that. Here we find the same generators J_σ, but in their discrete realization by matrices $\bar{J}_\sigma^{(k)}$; they are now shift operators on functions of the discrete row index n (so we distinguish them with overbars) and are written as

$$\bar{J}_0^{(k)}\psi(n) = (k + n)\psi(n), \tag{39}$$

$$\bar{J}_1^{(k)}\psi(n) = \frac{1}{2}\mu(k, n)\psi(n + 1) + \frac{1}{2}\mu(k, n - 1)\psi(n - 1), \tag{40}$$

$$\bar{J}_2^{(k)}\psi(n) = \frac{1}{2}\mu(k, n)\psi(n + 1) - \frac{1}{2i}\mu(k, n - 1)\psi(n - 1). \tag{41}$$

where

$$\mu(k, n) = [(n + 1)(2k + n)]^{1/2}. \tag{42}$$

Similarly, we can find $\bar{J}_{\pm}^{(k)} = \bar{J}_0^{(k)} \pm \bar{J}_1^{(k)}$ as in relations (28) and (29), where we note that neither of these operators is diagonal: Their eigenfunctions will satisfy second-order difference equations. This representation of the Lie algebra sp(2, $\Re$) of course also satisfies the commutation relations (30), and the quadratic invariant (31) is $(1/2)(1 - m^2) = k(1 - k)$. In particular, since $\bar{J}_0^{(k)}$ is represented here in its own eigenbasis, the fractional Hankel transform matrix (18) is diagonal:

$$\begin{aligned}(\mathcal{H}_{2k-1}^{\alpha} : \psi)(n) &= e^{i\pi k\alpha}[\mathcal{C}(\mathbf{H}^{\alpha})|^k : \psi](n) \\ &= e^{i\pi k\alpha}\sum_{n'\in\mathcal{Z}_0^+} D_{n,n'}^k \begin{bmatrix} \cos\frac{1}{2}\pi\alpha & \sin\frac{1}{2}\pi\alpha \\ -\sin\frac{1}{2}\pi\alpha & \cos\frac{1}{2}\pi\alpha \end{bmatrix} \\ &\quad \times \psi(n') \\ &= e^{-i\pi n\alpha}\psi(n).\end{aligned} \tag{43}$$

5. MEIXNER TRANSFORMS

The action of linear transformations $\mathcal{G} \in \mathrm{Sp}(2, \Re)$ on the vector space of the Lie algebra sp(2, $\Re$) is

$$J_{\vec{x}'} = \mathcal{G}J_{\vec{x}}\mathcal{G}^{-1}, \qquad J_{\vec{x}} = x_0J_0 + x_1J_1 + x_2J_2, \tag{44}$$

where the bilinear form $\chi(\vec{x}) = x_0^2 - x_1^2 - x_2^2 = \chi(\vec{x}')$ is invariant. The value of this invariant separates the 3D space $\vec{x} \in \Re^3$ into disjoint orbits, which we classify into strata: two sheets of hyperboloids, upper and lower cones, one-sheeted hyperboloids, and the origin point.

In Fig. 2 the generic upper hyperboloid is the first stratum of our interest; it is characterized by $\chi > 0$ and $x_0 > 0$. The operators $J_{\vec{x}}$ that belong to it (are compact and hence) generate SO(2) subgroups; this generic hyperboloid is therefore called the (upper) elliptic stratum. Such $J_{\vec{x}}$'s can be always transformed back to $\sqrt{\chi}J_0$ unitarily, and thus all elliptic operators have discrete spectra $\sqrt{\chi}(k + n)$, $n \in \mathcal{Z}_0^+$. The second stratum of interest is called the (upper) parabolic stratum, which is characterized by $\chi = 0$ and $x_0 > 0$ as the upper cone in Fig. 2. All operators in the parabolic stratum can be obtained unitarily from the generator J_+ of free flight (with helicity m) or from the generator of Gaussian lens phases, J_-; their spectra are continuous: $\rho = (1/2)x_0r^2 \in \Re_0^+$. (There is also the hyperbolic stratum with $\chi < 0$, where J_1 and J_2 lie, and whose spectra in D_k^+ are $\Re$.[13])

The Fourier transform (6) rotates Fig. 2 about the vertical J_0 axis by an angle of π, bringing J_- onto J_+ and J_+ onto J_-. When we compare this action with the 2×2 Hankel matrix representation (18) for $\alpha = 1, 2, 3, 4$, we can see that the latter covers 2:1 the rotation of the hyperboloids and cones in the figure (just as the dial of a clock covers twice the rotation of the Earth). The linear transformations of the $\Re^3$ space spanned by the $J_{\vec{x}}$'s actually form the group of $2 + 1$ pseudo-orthogonal matrices SO(2, 1), whose double cover is the group Sp(2, $\Re$). [In turn, Sp(2, $\Re$) is covered twice by the metaplectic group Mp(2, $\Re$), where k is a quarter-integer.] Two 2×2 matrices, $\pm\mathbf{M}$, map on the same 3×3 matrix that transforms the components of $\vec{x}$ to those of $\vec{x}'$ in Eqs. (44). (The rotation that brings J_1 onto J_2 is thus the square root of the Fourier transform, which intertwines the $\mathcal{L}^2(\Re)$ expansion in repulsive oscillator wave functions with the bilateral Mellin transform; see Ref. 11, Subsections 7.5.11–15.)

We call Meixner transforms $\mathcal{M}^{\zeta}$, $\zeta \in \Re$, the Sp(2, $\Re$) scale transformations [cf. Eq. (16) for $c = 0$, $a = e^{-\zeta/2}$]:

$$\mathcal{M}^{\zeta} = \exp(i\zeta J_2) = \mathcal{C}\begin{bmatrix} e^{-\zeta/2} & 0 \\ 0 & e^{\zeta/2} \end{bmatrix} = (\mathcal{M}^{-\zeta})^{-1}, \tag{45}$$

which map the generator J_0 to

$$\begin{aligned}J_{(\zeta)} &= \mathcal{M}^{\zeta}J_0\mathcal{M}^{-\zeta} \\ &= \cosh\zeta J_0 - \sinh\zeta J_1 \\ &= \tfrac{1}{2}e^{-\zeta}J_+ + \tfrac{1}{2}e^{\zeta}J_-.\end{aligned} \tag{46}$$

In D_k^+ the action of the Meixner transform on the canonical eigenvector set of $\bar{J}_0^{(k)}$, denoted by $\psi_n^{(k,0)}$, $n \in \mathcal{Z}_0^+$, is to map it on the eigenvector set of $\bar{J}_{(\zeta)}^{(k)}$,

$$\psi_n^{(k;\zeta)} = \mathcal{M}^{\zeta} : \psi_n^{(k;0)}. \tag{47}$$

The manifold of Meixner transforms is the line $(x_0, x_1, x_2) = (\cosh\zeta, -\sinh\zeta, 0) \in \Re^3$, $\zeta \in \Re$, on the upper hyperbolic sheet of Fig. 2.

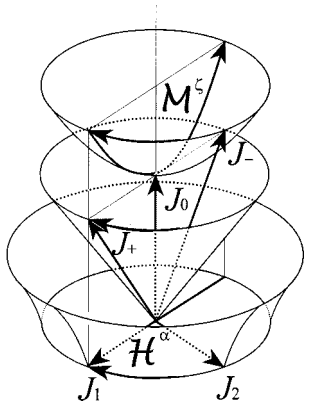

Fig. 2. Stratum surfaces of the generators $J_{\vec{x}}$ of Sp(2, $\Re$). Operators that lie on the same surface can be mapped onto each other by Sp(2, $\Re$) transformations. The $J_{(\zeta)}$ are obtained from J_0 through boosts generated by J_2; the heavy curve marked ζ is the manifold of Meixner transforms $\mathcal{M}^{\zeta}$. The fractional Hankel–Meixner transforms $\mathcal{H}^{\alpha}$ are rotations, generated by J_0, around the vertical axis of the figure by $\pi\alpha$.

The coordinates of a vector $f \in \ell^2$ in the basis $\{\psi_n^{(k;\zeta)}\}_{n=0}^{\infty}$ are $f^{(k;\zeta)}(n') = (\psi_{n'}^{(k;\zeta)}, f)_{\ell^2}$, where the upper indices $(k;\ \zeta)$ of $f(n')$ are kept for reference in case we use more than one eigenbasis. In particular, the waveguide normal modes $\psi_n^{(k;0)}$ (whose coordinates in the standard J_0 eigenbasis are simply $\delta_{n,n'}$) will, in the basis (47), have the real coordinates found in Eq. (34), namely,

$$\begin{aligned}\psi_n^{(k;0,\zeta)}(n') &= (\psi_{n'}^{(k;\zeta)}, \psi_n^{(k;0)})_{\ell^2} \\ &= (\psi_{n'}^{(k;0)}, \mathcal{M}^{-\zeta} : \psi_n^{(k;0)})_{\ell^2} \\ &= D^k_{n',n}\begin{bmatrix} e^{\zeta/2} & 0 \\ 0 & e^{-\zeta/2}\end{bmatrix} \\ &= \frac{(-1)^n\Gamma(2k+n+n')}{[n!n'!\Gamma(2k+n)\Gamma(2k+n')]^{1/2}}\,\frac{\tanh^{n+n'}(1/2)\zeta}{\cosh^{2k}(1/2)\zeta,}F\left[\begin{matrix}-n, & -n' \\ 1-2k-n-n'\end{matrix}; \coth^2\tfrac{1}{2}\zeta\right], \quad (48)\end{aligned}$$

$$= \psi_n^{\mathrm{M}}(n';\ 2k, \tanh^2\tfrac{1}{2}\zeta) = d^k_{k+n',k+n}(\zeta) = (-1)^{n'}\psi_{n'}^{(k;-\zeta,0)}(n), \quad (49)$$

where $d^k_{m',m}(\zeta)$ are the Bargmann d's reported in Ref. 2 and we use the notation ψ^{M} introduced in Ref. 7 for the Meixner functions. For $\beta = 2k$ and $\gamma = \tanh^2(1/2)\zeta$, these are

$$\begin{aligned}\psi_n^{(k;0,\zeta)}(\xi) &= \psi_n^{\mathrm{M}}(\xi;\ \beta,\ \gamma) \\ &= \left[\frac{\gamma^{n+\xi}(1-\gamma)^{\beta}(\beta)_n(\beta)_{\xi}}{n!\Gamma(\xi+1)}\right]^{1/2} M_n(\xi;\ \beta,\ \gamma),\end{aligned} \quad (50)$$

with $(\beta)_{\xi} = \Gamma(\beta+\xi)/\Gamma(\beta)$, and where

$$\begin{aligned}M_n(\xi;\ \beta,\ \gamma) &= F\left[\begin{matrix}-n,\ -\xi \\ \beta\end{matrix};\ 1-\frac{1}{\gamma}\right] \\ &= \frac{(\beta+\xi)_n}{(\beta)_n}F\left[\begin{matrix}-n, -\xi \\ 1-\beta-n-\xi\end{matrix};\ \frac{1}{\gamma}\right]\end{aligned} \quad (51)$$

are the *Meixner polynomials*.[19] These polynomials are real and well defined for continuous $\xi > -1$, $\beta > 0$, and $0 < \gamma < 1$. The Meixner functions are analytic on the plane, except for a branch cut on the negative real axis. We can check that, as $\gamma,\ \zeta \to 0$, $\psi_n^{(k;0,\zeta)}(n') \to \delta_{n,n'}$ on $\mathcal{Z}_0^+$.

From the unitarity of the representation matrices follows the orthogonality and completeness of the Meixner functions over the integers $\xi \in \mathcal{Z}_0^+$:

$$\begin{aligned}\sum_{\xi\in\mathcal{Z}_0^+}\psi_n^{\mathrm{M}}(\xi)\psi_{n'}^{\mathrm{M}}(\xi) &= \delta_{n,n'}, \\ \sum_{n\in\mathcal{Z}_0^+}\psi_n^{\mathrm{M}}(\xi)\psi_n^{\mathrm{M}}(\xi') &= \delta_{\xi,\xi'},\end{aligned} \quad (52)$$

where to streamline the notation we have suppressed the common parameters $\beta,\ \gamma$ or $(k;\ 0,\ \zeta)$. The first parameter $2k = \beta = |m| + 1$ is the strength m of the helicity core in the waveguide (21). The second parameter $\gamma = \tanh^2(1/2)\zeta \in [0, 1)$ is a scale for the waveguide width, as can be seen from Eq. (46) in the realization [relations (28) and (29)]. The index $n \in \mathcal{Z}_0^+$ numbers the waveguide eigenmodes of J_0 in D_k^+.

The limit from the discrete to the continuum is shown in Fig. 3, where $J_{(\zeta)}$ of Eq. (46) grows and approaches asymptotically the cone as $\zeta \to \infty$. To have a line of vectors with limit J_-, we can downsize the $J_{(\zeta)}$'s by a factor of $2e^{-\zeta}$, so that, when $\zeta \to \infty$,

$$K_{(\zeta)} = 2e^{-\zeta}J_{(\zeta)} = J_- + e^{-2\zeta}J_+ \to J_-. \quad (53)$$

In D_k^+ the spectrum of $\hat{K}_{(\zeta)}^{(m)}$ is $\kappa_n^{|m|} = 2e^{-\zeta}(k+n)$, $n \in \mathcal{Z}_0^+$; with increasing ζ, this set of points become dense in $\rho = \Re_0^+$, which is the spectrum of the limit $\hat{J}_-^{(m)}$ [see relation (29)]. Since the spectrum of $\hat{J}_-^{(m)}$ is identified with $(1/2)r^2$, its covariant discretization (for any finite ζ) entails identifying the discrete spectrum with the set of discrete sensor radii $(1/2)r_n^2$. We match them at zero and propose

$$2e^{-\zeta}n = \tfrac{1}{2}r_n^2 \leftrightarrow \rho = \tfrac{1}{2}r^2. \quad (54)$$

The values of the discrete radial coordinate with scale ζ are thus

$$r_n = 2e^{-\zeta/2}\sqrt{n} \leftrightarrow r, \qquad n = \tfrac{1}{4}e^{\zeta}r_n^2. \quad (55)$$

Let us now examine the circles of sensors with these radii r_n in the array of Fig. 1(c). Two consecutive circles enclose annuli of equal area $4\pi e^{-\zeta}$; they come closer together as do Newton rings. When the scaling parameter ζ grows, the radii in the array shrink by a factor of $e^{-\zeta/2}$; a fixed radius r will be matched by a sensor circle $r_{n'}$

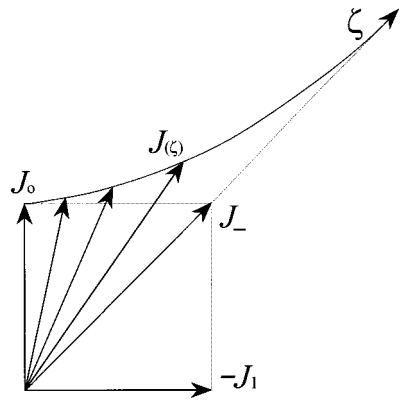

Fig. 3. As ζ grows, $J_{(\zeta)}$ asymptotically approaches the direction of J_-; a change of scale by $2e^{-\zeta}$ is needed to make the vectors $K_{(\zeta)}$ coincide with the desired limit.

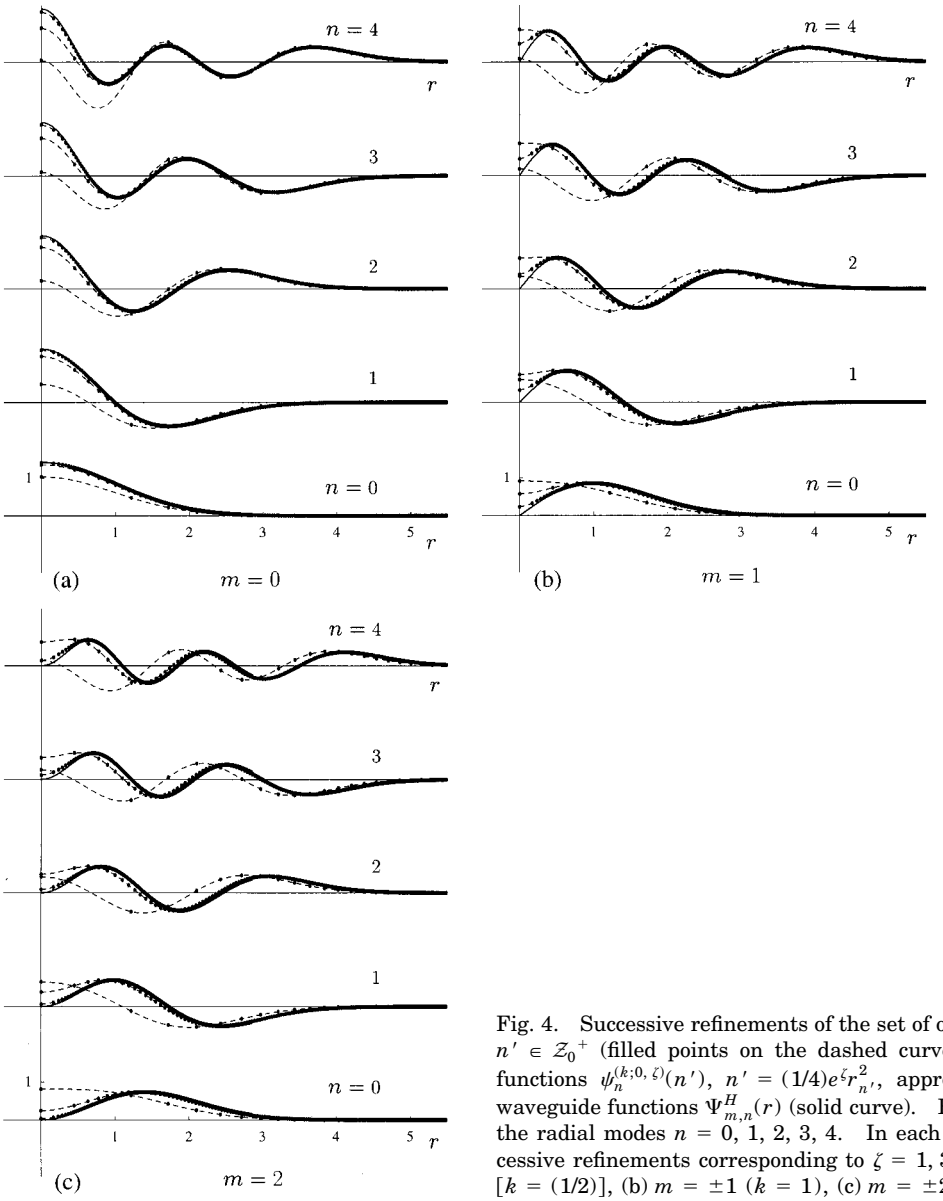

Fig. 4. Successive refinements of the set of orthogonality points $n' \in \mathcal{Z}_0^+$ (filled points on the dashed curves) of the Meixner functions $\psi_n^{(k;0,\zeta)}(n')$, $n' = (1/4)e^{\zeta}r_{n'}^2$, approximate the radial waveguide functions $\Psi_{m,n}^H(r)$ (solid curve). From bottom to top, the radial modes $n = 0, 1, 2, 3, 4$. In each plot there are successive refinements corresponding to $\zeta = 1, 3, 5, \infty$. (a) $m = 0$ $[k = (1/2)]$, (b) $m = \pm 1$ $(k = 1)$, (c) $m = \pm 2$ $[k = (3/2)]$.

numbered by ever larger n''s. Thus in the limit $\zeta \to \infty$ the discrete optical world becomes a continuum, while the action of linear optical systems is smoothly preserved. Indeed, the following limit of the Meixner to the Laguerre polynomials is known[19]:

$$\lim_{\zeta\to\infty} M_n(e^{\zeta}\rho;\ \beta,\ 1 - 2e^{-\zeta}) = \frac{n!}{(\beta)_n} L_n^{\beta-1}(2\rho), \qquad (56)$$

and it is valid for continuous $\rho \geqslant 0$. For fixed r and for the integer $n' = \xi$ that grows with ζ as $(1/4)e^{\zeta}r^2$, the limit for the Meixner functions (50) is the Laguerre functions (23) of the continuous waveguide[16]:

$$\lim_{\zeta\to\infty} \frac{1}{\sqrt{2}} e^{\zeta/2}\psi_n^{(k;0,\zeta)}\left(\frac{1}{4}e^{\zeta}r^2\right) = \Psi_{m,n}^{\mathrm{H}}(r). \qquad (57)$$

In Fig. 4 we plot this limit for several values of m and n.

Note that the limit (57) is equally valid if, to the argument $(1/4)e^{\zeta}r^2$ of the Meixner function, we add a finite constant c, so that instead of relation (55) we would have the raddi $r_n^{\mathrm{c}} = 2e^{-\zeta/2}\sqrt{c+n}$, and there would be an innermost circle of sensors r_0^c. This obvious remark points to the fact that the identification (55) between labels and radii of sensor circles is not unique. A multiplicity of discrete systems coalesces to the common continuous limit. In this context we should point out that, had we used the straightforward identification choice $\kappa_n^{|m|} \leftrightarrow \rho$ in place of relation (54), the radii of the sensor circles would be $r_{k+n} = 2e^{-\zeta/2}\sqrt{k+n}$, falling into two families for even and odd helicities (integer and half-integer k), and each partial helicity wave field would be sensed only from r_k outward. This choice for the radial variable would complicate our transform formulas in Section 7, but we should acknowledge it as a possible alternative.

6. HANKEL–MEIXNER TRANSFORMS

We call fractional Hankel–Meixner transform $\mathcal{H}^{\alpha}$ the canonical rotation $\mathrm{SO}(2) \subset \mathrm{Sp}(2, \Re)_r$ by an angle $(1/2)\pi\alpha$

around the J_0 axis; on the vectors in Fig. 2 this corresponds to a rotation by $\pi\alpha$ in the direction shown by the arrows. As we saw, this operation in the eigenbasis of J_- is represented by the radial canonical integral kernel (15), whereas, in the eigenbasis of J_0 [or of any $J_{(\zeta)}$ in the elliptic stratum], the Hankel–Meixner transform is represented by a lower-bound, infinite matrix. In the limit $\zeta \to \infty$ the Hankel–Meixner transform becomes the usual, continuous fractional Hankel transform (19).

We indicate by $\mathbf{H}^{\alpha;|m|,\zeta} = \|H^{\alpha;|m|,\zeta}_{n,n'}\|$ the fractional Hankel–Meixner transform matrix (of power α, helicity $|m| = 2k - 1$, and scaling ζ), which represents $\mathcal{H}^{\alpha}|^k = \exp[-i\pi\alpha(\bar{J}_0^{(k)} - k1)]$ in the eigenbasis of $\bar{J}_{(\zeta)}^{(k)}$. The matrix elements can be found from Eqs. (24) and (43) by use of orthonormality and completeness properties for the bases, to express them as a bilinear Namias generating function,[20] namely,

$$H^{\alpha;2\,:\,\kappa-1,\zeta}_{n,n''} = (\psi_n^{(k;\zeta)},\ \mathcal{H}^{\alpha}\,:\,\psi_{n''}^{(k;\zeta)})_{\ell^2} = \sum_{n'\in\mathcal{Z}_0^+} \psi_n^{(k;\zeta)}(n')e^{-i\pi\alpha n'}\psi_{n''}^{(k;\zeta)}(n'). \quad (58)$$

This matrix is unitary: $H^{-\alpha;|m|,\zeta}_{n,n'} = (H^{\alpha;|m|,\zeta}_{n',n})^*$. As in Section 5, henceforth we should use $n' = (1/4)e^{\zeta}r_{n'}^2$ when referring to the radial coordinate on the screen for each helicity wave field. The bilinear generating function (58) can be evaluated easily by use of the representation property

$$\begin{aligned} e^{-i\pi k\alpha}H^{\alpha;|m|,\zeta}_{n,n'} &= (\psi_n^{(k;\zeta)}, \exp(i\pi\alpha J_0\,:\,\psi_{n'}^{(k;\zeta)}))_{\ell^2} \\ &= \left(\psi_n^{(k;0)},\ \mathcal{C}\begin{bmatrix} e^{\zeta/2} & 0 \\ 0 & e^{-\zeta/2}\end{bmatrix}\begin{bmatrix} \cos\tfrac{1}{2}\pi\alpha & -\sin\tfrac{1}{2}\pi\alpha \\ \sin\tfrac{1}{2}\pi\alpha & \cos\tfrac{1}{2}\pi\alpha\end{bmatrix}\begin{bmatrix} e^{-\zeta/2} & 0 \\ 0 & e^{\zeta/2}\end{bmatrix}\mathcal{C}\,:\,\psi_{n'}^{(k;0)}\right)_{\ell^2} \\ &= D^k_{n,n'}\begin{bmatrix} \cos\tfrac{1}{2}\pi\alpha & -e^{\zeta}\sin\tfrac{1}{2}\pi\alpha \\ e^{-\zeta}\sin\tfrac{1}{2}\pi\alpha & \cos\tfrac{1}{2}\pi\alpha\end{bmatrix}. \end{aligned} \quad (59)$$

The full expression is given in Appendix A, Eq. (A2), for $\theta = (1/2)\pi\alpha$.

The fractional $(\alpha;\ |m|,\ \zeta)$–Hankel–Meixner transform of a given half-infinite data set $f(n')$, $n' \in Z_0^+$, $f \in \ell^2$, measured at the radii $r_{n'} = 2e^{-\zeta/2}\sqrt{n'}$, is

$$(\mathcal{H}^{\alpha}|^k\,:\,f)(n)^{(\zeta)} = \sum_{n'\in\mathcal{Z}_0^+} H^{\alpha;|m|,\zeta}_{n,n'}f(n'). \quad (60)$$

The representing Hankel–Meixner matrices form a cyclic group in α:

$$\sum_{n'\in\mathcal{Z}_0^+} H^{\alpha_1;|m|,\zeta}_{n,n'}H^{\alpha_2;|m|,\zeta}_{n',n''} = H^{\alpha_1+\alpha_2;|m|,\zeta}_{n,n''}. \quad (61)$$

The fractional Hankel transforms count this cycle in α modulo 2; the phase in definition (59) guarantees that $H^{0;|m|,\zeta}_{n,n'} = \delta_{n,n'} = H^{2;|m|,\zeta}_{n,n'}$. When the parameter ζ is zero the eigenbasis is that of J_0, where Eq. (35) holds, namely, $H^{\alpha;|m|,0}_{n,n'} = e^{-i\pi n\alpha}\delta_{n,n'}$. Finally, in the limit $\zeta \to \infty$, we find from Eq. (57) that the Hankel–Meixner matrix (59) converges to the Hankel transform kernel (19):

$$\lim_{\zeta\to\infty} H^{\alpha;|m|,\zeta}_{n,n'} = H^{\alpha}_m(r,r') = e^{i\pi k\alpha}C^{(m)}_{H^{\alpha}}(r,r'), \qquad n \approx \tfrac{1}{4}e^{\zeta}r^2, \qquad n' \approx \tfrac{1}{4}e^{\zeta}r'^2. \quad (62)$$

7. DISCRETIZATION OF THE POLAR SCREEN

We return to the original problem of placing sensor points in concentric circles on the screen. In Section 2 the 2D continuous Fourier transform (6) was rewritten in Eq. (8) as a sum of Hankel transforms $(\mathcal{H}_m\,:\,\psi_m^{\mathrm{H}})(r)$, $m \in \mathcal{Z}$, in the radial coordinate $r \in \Re_0^+$ and was multiplied by phases $e^{im\theta}$ in the angular coordinate $\theta \in \mathcal{S}^1$. To discretize the radial coordinate we straightforwardly replace the radial Hankel transforms with the discrete Hankel–Meixner transforms in D_k^+, $(\mathcal{H}^{\alpha}|^k\,:\,\bar{\psi}_m^{\mathrm{H}})(n')^{(\zeta)}$ of the same power $(\alpha = 1)$ and a fixed scale parameter ζ. In the subgroup reduction (2), the representations $\pm m$ of $\mathrm{SO}(2)_{\theta}$ and k of $\mathrm{Sp}(2,\Re)_r$ essentially determine each other through Eqs. (32) and are said to be conjugate within the metaplectic representation of $\mathrm{Sp}(4,\ \Re)$.

The expression that takes the place of Eqs. (8)–(10) in the case of Fourier decomposition $\mathcal{F}$ of the wave field $\psi(n,\ \theta)$ (on the nth concentric circle and of continuous angle $\theta \in \mathcal{S}^1$) will be denoted by $\bar{\mathcal{F}}$ (because it acts on one discrete and one continuous argument), and it is

$$\psi(n,\ \theta) = (\bar{\mathcal{F}}\,:\,\psi^{\mathrm{H}})(n,\ \theta) = \sum_{m\in\mathcal{Z}} \frac{e^{im\theta}}{\sqrt{2\pi}}(-i)^m \sum_{n'\in\mathcal{Z}_0^+} H^{1;|m|,\zeta}_{n,n'}\psi^{\mathrm{H}}_m(n'). \quad (63)$$

But now assume that on each circle n we can measure only the wave field at a discrete, equidistant set of N sensors labeled by integer ℓ modulo N ($\ell \in \mathcal{Z}_N$), at angles

$$\theta_n \in \{\theta_{n,0},\ \theta_{n,1},\ldots,\ \theta_{n,N-1}\}, \qquad \theta_{n,\ell} = \theta_{n,0} + 2\pi\ell/N, \quad (64)$$

where the number of sensors $N = N(n)$ can vary with the chosen circle as well as with the starting angle $\theta_{n,0}$. In Fig. 1(c) we show the array of sensors on the screen corresponding to $N = 7$, $\theta_{n,0} = 2\pi s n$, with step $s = 0.1$. To invert Eq. (63), we can sum only over the values of $\psi(n, \ell) = \psi(n, \theta_\ell)$ at the sensor points through the finite Fourier transform, so we have a finite sum over ℓ's given by

$$\frac{\exp(-im\theta_{n,0})}{N(n)} \sum_{\ell \in \mathcal{Z}_N} \exp(-2\pi i m \ell / N)\, \psi(n, \ell) = \frac{(-i)^m}{\sqrt{2\pi}} \sum_{n' \in \mathcal{Z}_0^+} H^{1;|m|,\zeta}_{n,n'} \psi^{\mathrm{H}}_m(n'). \quad (65)$$

The left-hand side of this equation (L) obeys the periodicity condition $L(n, m + N) = \exp(-iN\theta_{n,0}) L(n, m)$; we may thus replace the infinite sum over $m \in \mathcal{Z}$ in Eq. (63) with a correspondingly finite sum over $m \in \mathcal{Z}_N$. This implies that, at a given circle n, the number of helicity components that we measure will not be greater than that of the N sensors on that circle. The restriction is benign, since it is well known that (in the usual norm of wave-field energy) truncation in an orthogonal basis yields the minimum-energy continuous solution that matches the values of the true wave field at the sensor points.[21]

The fundamental range of $m \in \mathcal{Z}_N \subset \mathcal{Z}$ must be specified because it determines a finite range for the Bargmann index k of the Hankel–Meixner transforms. For odd N we take $-(1/2)(N-1) \leqslant m \leqslant (1/2)(N-1)$, while for even N we may take either $-(1/2)N + 1 \leqslant m \leqslant (1/2)N$ or the reflected range. It seems convenient to consider the simpler case of odd $N(n)$, because then one can pair conjugate phases in θ with real trigonometric functions. The Fourier synthesis and analysis of a wave field on discrete radial and discrete angular coordinates (indicated by a double overbar) are thus, respectively,

$$\psi(n, \ell) = (\bar{\bar{\mathcal{F}}} : \psi^{\mathrm{H}})(n, \theta_\ell) = \frac{1}{\sqrt{2\pi}} \sum_{m \in \mathcal{Z}_{N(n)}} (-i)^m \exp(im\theta_{n,\ell}) \times \sum_{n' \in \mathcal{Z}_0^+} H^{1;|m|,\zeta}_{n,n'} \psi^{\mathrm{H}}_m(n'), \quad (66)$$

$$\psi^{\mathrm{H}}_m(n') = (\bar{\bar{\mathcal{F}}}^{-1} : \psi)_m(n') = \sqrt{2\pi} i^m \sum_{n \in \mathcal{Z}_0^+} \frac{1}{N(n)} (H^{1;|m|,\zeta}_{n,n'})^* \times \sum_{\ell \in \mathcal{Z}_{N(n)}} \exp(-im\theta_{n,\ell}) \psi(n, \ell), \quad (67)$$

for every value of the scaling parameter ζ. We have taken care to indicate the circle (n or n') to which N and $\theta_{n,\ell}$ belong. In particular, the point $n = 0$ at the center of the array should be single sensor $N(0) = 1$, and, since $\mathcal{Z}_1 = \{0\}$, both ℓ and m can only be zero. The synthesis of the wave field (66) at the center of the waveguide and the analysis of the zero-helicity component (67) are, respectively,

$$\psi_n(0,0) = \frac{1}{\sqrt{2\pi}} \sum_{n' \in \mathcal{Z}_0^+} H^{1;0,\zeta}_{n,n'} \psi^{\mathrm{H}}_0(n'),$$

$$\psi^{\mathrm{H}}_0(n') = \sqrt{2\pi} \sum_{n \in \mathcal{Z}_0^+} \frac{1}{N(n)} (H^{1;0,\zeta}_{n,n'})^* \sum_{\ell \in \mathcal{Z}_{N(n)}} \psi(n, \ell). \quad (68)$$

8. SPIRALING COHERENT STATES

The evolution of discrete wave fields $\psi(n, \ell)$ along a waveguide of length α, in units where $\alpha = 4$ is one oscillation length, is due to the action of the canonical transform operator $\mathcal{C}(\mathbf{H}^\alpha) = \exp(-i\pi\alpha J_0)$. This rotates the optical phase-space planes (q_x, p_x) and (q_y, p_y) jointly by $(1/2)\pi\alpha$, while the $\mathfrak{R}^3$ space of Fig. 2 is rotated by double the angle, $\pi\alpha$. Now, in accordance with Eq. (59), during evolution along the waveguide, each helicity summand of Eq. (66) is multiplied by the phase factor $\exp(-i\pi k\alpha)$, $k = (1/2)(|m| + 1)$, times the corresponding Hankel–Meixner transform of power α. In the same equation the angular dependence on $\theta_{n,\ell}$ is contained in the factor $\exp[(2\pi i m \ell / N(n)]$. For $m = \pm|m|$ and for every circle n, the two phases multiply, and their angular dependence results in the phase $\exp[-i(1/2)\pi\alpha] \exp\{(2\pi i m/N)[\ell \mp (1/4)N\alpha]\}$—as if the field value at ℓ had been rotated continuously to $\ell \mp (1/4)N\alpha$.

The $\mathrm{SO}(2)_\theta$ rotation of the discrete angular coordinate ℓ, as the screen advances along the waveguide, is clockwise for all $m > 0$ helicity components and counterclockwise for $m < 0$ and is ignorable for axis-symmetric wave fields $m = 0$. Since the angular dependence of each helicity-m wave field (at every circle n) is $\sim\exp(im\theta_{n,\ell})$, each partial wave field completes m turns in the common period $\alpha = 4$. This is important because it implies that the Perelomov-type[22] and the Barut–Girardello-type,[23] radial coherent states of each helicity pair $\pm m$ will have an angular dependence of the general form $\sim\cos(m\theta_{n,\ell} + \phi)$, with $2|m|$ extrema around the circle. This will move coherently in both the radial and the angular coordinates, drawing out a $2|m|$-fold helix along the waveguide axis, packed around the classical elliptic-cylinder trajectories. In Ref. 7 we built the two types of coherent states for the Meixner radial oscillator, which are necessary for the further characterization of coherence phenomena in discrete polar coordinates.

In a separate study we must analyze the numerical faithfulness with which single-helicity coherent motion is rendered on discrete screens of sensors, as was done for the Kravchuk oscillator (planar waveguide) in Ref. 24, and also the case in which several helicities combine to form one angular wave packet. Nevertheless, we must emphasize here that, in different discretization schemes, a smooth angular motion cannot be obtained if at some step one replaces $\partial^2/\partial\theta^2$, in the angular part of an evolution equation, with the second-difference operator in θ_ℓ, because such a system will not have a common fundamental period.

9. LINEAR CANONICAL TRANSFORMATIONS

The process of discretization of the 2D fractional Fourier transform that we detailed above can be generalized from waveguide motion to all axis-symmetric linear optical transformations $\mathbf{M} \in \mathrm{Sp}(2, \Re)$ in a covariant way. The canonical transform kernel [Eqs. (12)–(15)] corresponds to the matrix kernel in the discrete J_0 basis of $\zeta = 0$, which is given in Eqs. (34)–(36).

With the same change of basis as in Section 6, we can find the action of the optical system on discrete sensor arrays with different scale parameters ζ. A linear optical system $\mathbf{M}$ acts on discrete wave fields $\psi(n, \ell)$, sensed on arrays such as Fig. 1(c) and with sensors numbered by $(n, \theta_{n,\ell})$ as detailed in Section 7, through

$$(\mathcal{C}(\mathbf{M})|^k\colon \psi)(n, \ell)^{(\zeta)} = \frac{1}{\sqrt{N(n)}} \sum_{m \in \mathcal{Z}_{N(n)}} \exp(im\theta_{n,\ell}) \times \sum_{n' \in \mathcal{Z}_0^+} \mathcal{C}^{(k;\zeta)}_{n,n'}(\mathbf{M})\psi(n', m), \tag{69}$$

where, as usual, $k = (1/2)(|m| + 1)$. The transform kernel is a matrix whose elements are

$$\begin{aligned} \mathcal{C}^{(k;\zeta)}_{n,n'}\begin{bmatrix} a & b \\ c & d \end{bmatrix} &= \left(\psi^{(k;\zeta)}_n, \mathcal{C}\begin{bmatrix} a & b \\ c & d \end{bmatrix} : \psi^{(k;\zeta)}_{n'} \right) \\ &= \left(\psi^{(k;0)}_n, \mathcal{C}\begin{bmatrix} e^{\zeta/2} & 0 \\ 0 & e^{-\zeta/2} \end{bmatrix}\begin{bmatrix} a & b \\ c & d \end{bmatrix} \times \begin{bmatrix} e^{-\zeta/2} & 0 \\ 0 & e^{\zeta/2} \end{bmatrix} : \psi^{(k;0)}_{n'} \right) \\ &= D^k_{n,n'}\begin{bmatrix} a & e^{\zeta}b \\ e^{-\zeta}c & d \end{bmatrix}. \end{aligned} \tag{70}$$

This generalizes Eqs. (58) and (59) for $\mathbf{M} = \mathbf{H}^1$ and $\psi(n', m) = \psi^{\mathrm{H}}_m(n')$. In this way linear axis-symmetric optical systems [elements of $\mathrm{Sp}(2, \Re)_r$] map unitarily square-summable functions $\psi(n, \ell)$ [on discrete circles n of radii $r_n = 2e^{-\zeta}\sqrt{n}$ and discrete angles $\theta_{n,\ell} = \theta_{n,0} + 2\pi\ell/N(n)$] to other such functions, on the same array of points.

10. CONSIDERATIONS ON DISCRETE PHASE SPACE

It may seem inconvenient that, as n grows, the radii r_n come closer together. The reason that a covariant discretization forces us to an infinite sequence of ever-closer circles of sensors is that the linear spectrum of a $K_{(\zeta)}$ [relation (53)] is identified as $(1/2)r_n^2$, which is the physical interpretation of the spectrum of J_-. This spacing ensures that the action of Gaussian lenses, which multiply the wave field by a quadratic phase $\exp(i\gamma r_{n'}^2)$, is faithful.

A polar array of points can look homogeneous from a distance, or it can exhibit a radial density determined by the number of points $N(n)$ on each circle. To estimate this quantity, consider a surface element on the plane, $\mathrm{d}q_x\mathrm{d}q_y = r\mathrm{d}r\mathrm{d}\theta = (1/2)\mathrm{d}r^2\mathrm{d}\theta$. Since our array has radii $(1/2)r_n^2 = 2e^{-\zeta}n$, the discrete surface element is $2e^{-\zeta}\Delta n\,\Delta\theta_\ell$, with $\Delta n = 1$ and $\Delta\theta_\ell = 2\pi/N(n)$; it is thus $4\pi e^{-\zeta}/N(n)$. When $N(n)$ is a constant (i.e., when the array has the same number of sensors on each circle) the finite element is constant over the screen. This is the case in Fig. 1(c).

The points of the 2D sensor array (n, ℓ) are the position coordinates for the phase space of this discrete axis-symmetric optical model. Through the Fourier transformation (69) we have found the canonically conjugate momentum coordinates as points (n', m) arranged in the same fashion. If we follow the construction of phase space for finite quantum mechanics that was set forth by Wootters[25] or that for the cyclic case, used by Hakioğlu in Ref. 26, where both position and momentum are discrete points (on a straight segment or on a circle, respectively), we are led to a phase space that is the direct product of the sensor pattern of Fig. 1(c) with itself. The geometric rays, corresponding to the phase-space points, are straight lines through the array, pointing in (paraxial) directions given by an array of the same kind; in a semiclassical interpretation the wave-field value at one sensor will be the sum over all ray directions.

To represent a beam on this discrete phase space one would have to propose an appropriate 4D discrete Wigner function,[25,26] of which the square wave field would be one of several possible marginal distributions (projections).[27] Using it, one should expect to see with clarity the geometric action of linear optical systems, in particular, the fractional Fourier transform. We have not found such a discrete Wigner function. What we have up to this point are faithful maps among functions of the sampled values of the wave field, where canonicity may be subsumed by the unitarity properties of the representation of $\mathrm{Sp}(2, \Re)$.

We want to set forth another interpretation of phase space, following the geometric analysis of ray trajectories in 3D waveguides that was developed in Ref. 28 and of 2D (planar) finite waveguide systems of N sensors that was given in Ref. 29. In the latter study we proposed the definition of a (meta-) phase space $\vec{x} \in \Re^3$, based on the spin group SU(2), of classical coordinates of position, momentum, and oscillator mode. There is a Wigner operator $\mathcal{W}(\vec{x})$, which is essentially the covariant Fourier transform of the group action (and an element of the group ring; see Refs. 29 and 30). Signals in the planar waveguide are vectors $\psi \in \Re^N$, whose coordinates (sensor values) in Dirac's notation are $\psi(n) = \langle n|\,\psi\rangle$, where $\{|n\rangle\}_{n=0}^{N-1}$ is a suitable, complete orthonormal basis. In that context the interplay of two signals ϕ, ψ can be depicted on $\Re^3$ by their matrix element of the Wigner operator,

$$W(\phi, \psi; \vec{x}) = \langle \phi|\mathcal{W}(\vec{x})|\,\psi\rangle, \tag{71}$$

which is the covariant Wigner function in SU(2). When $\phi = \psi$ this results in plots whose density is found to be closely concentrated around the surface of a sphere of radius $|\vec{x}| \approx (1/2)N$. (From this Wigner function on $\Re^3$ follows the Wigner function for spin systems on the sphere, which was developed by Agarwal[31] and by Várilly and Gracia-Bondía[31]; the relation has been established in Ref. 32.)

In the present case the group is that of linear optical systems, $\mathrm{Sp}(2, \Re)$, generated by the operators of squared

position J_-, squared momentum J_+, and scaling J_2. We have credible indications that one can set up in $\mathfrak{R}^3$ an Sp(2, $\mathfrak{R}$)-covariant Wigner function[30] in terms of the corresponding classical coordinates $x_- = \mathbf{q}^2$, $x_+ = \mathbf{p}^2$, and $x_2 = \mathbf{q} \cdot \mathbf{p}$, where the partial wave fields of each helicity m will be represented by density plots, concentrated around the surface of the hyperboloid $\mathbf{q}^2\mathbf{p}^2 - (\mathbf{q} \cdot \mathbf{p})^2 = (\mathbf{q} \times \mathbf{p})^2 \approx (1/2)m^2$ and determined by their Petzval–Casimir operator (31). Beams containing all helicities will be represented on the interior of the upper cone in Fig. 2. This Wigner function, being invariant under rotations around the physical waveguide axis, will thus reflect the rotation-independent features of the wave fields; it will be covariant with the action of linear axis-symmetric optical systems, which act linearly on the $\mathfrak{R}^3$ coordinates of meta-phase-space, preserving the hyperbolic metric.

In contradistinction to SU(2), however, Sp(2, $\mathfrak{R}$) is endowed with three distinct subgroups; here we used the countable eigenbasis of $K_{(\zeta)}$ [relation (53)], and the continuous (generalized) eigenbasis of J_-, in all D_k^+ (Bargmann's discrete) representations. In Dirac's very succinct notation let us indicate the bases by $\{|n\rangle^{(\zeta)}\}_{n \in \mathcal{Z}_0^+}$ and $\{|r\rangle\}_{r \in \mathcal{R}_0^+}$, respectively. [We recall that the overlap $\langle r|n\rangle^{(0)}$ for $K_{(0)} = J_0$ is the Laguerre function (23); for the general-ζ case, we can rescale r with Eq. (16) or with the Meixner transform (47).] One signal ψ in the helicity-m wave field is given in the countable bases by the discrete coordinates $\psi(n) = {}^{(\zeta)}\langle n|\,\psi\rangle$ or, equivalently, by its continuous coordinates $\psi(r) = \langle r|\,\psi\rangle$. But note that the Wigner function defined in Eq. (71) is independent of the basis. Introducing the resolution of the identity (in any Dirac-complete basis) on both sides of the operator in that definition, we can express the Sp(2, $\mathfrak{R}$)-covariant Wigner function as

$$W(\phi, \psi; \vec{x}) = \sum_{n \in \mathcal{Z}_0^+} \sum_{n' \in \mathcal{Z}_0^+} [{}^{(\zeta)}\langle n|\,\phi\rangle]^* \times {}^{(\zeta)}\langle n|\mathcal{W}(\vec{x})|n'\rangle^{(\zeta)}\ {}^{(\zeta)}\langle n',\psi\rangle, \tag{72}$$

$$= \int_{\mathfrak{R}_0^+} \mathrm{d}r \int_{\mathfrak{R}_0^+} \mathrm{d}r' (\langle r|\,\phi\rangle)^* \langle r|\mathcal{W}(\vec{x})|r'\rangle \langle r'\psi\rangle. \tag{73}$$

Therefore, under covariant discretization, the covariant Wigner function of the discretized wave field will be the same for all ζ as well as for their continuum limit. The analytic form of the Sp(2, $\mathfrak{R}$)-covariant Wigner function is not yet available, but its compatibility with this discretization of signals is clear. Finally, the classical limit $k \to \infty$ of this function should yield ray trajectories such as those sketched in Ref. 28.

11. CONCLUSIONS

In this paper we have applied classical results of the group of 2×2 matrices to build a model of discrete optical systems with axial symmetry and with the proper continuum limit. We provided orthonormal bases of functions on polar arrays of sensors on which the representation of $\mathrm{Sp}(2, \mathfrak{R})_r$ is defined, faithful, and unitary. This group contains, in particular, the fractional Hankel–Meixner transform cycle of a waveguide and its limit, the canonical fractional Hankel transform. Discrete cylindrical waveguides possess coherent states.

Appearances notwithstanding, the group of 2×2 matrices has a very rich structure. Here we have used its D_k^+ representations by matrices in eigenbases of operators that are only in the upper cone of Fig. 2. In the complementary hyperbolic stratum of one-sheeted hyperboloids lies the scaling operator J_2, for example, whose eigenfunctions $\{r^{-(1/2)+i\lambda}\}_{\lambda \in \mathfrak{R}}$ form the Mellin transform kernel.[13] Furthermore, the D_k^+ representations of 2×2 matrices can be extended to a complex semigroup that includes Gaussian diffusion (as in heat),[12] which models linear systems with loss. Moreover, besides the Bargmann D_k^+ discrete representations for right-moving wave fields, one has also the upper-bound $D_{\bar{k}}^-$ representation series, associated with the lower cone of Fig. 2, where the spectrum of J_0 is inverted and which evidently applies to left-moving fields. Nonlinearities, too, have been handled for SU(2)-optical systems, in Ref. 33 for a quantum-optical Kerr medium. In our model of axis-symmetric linear systems the interesting nonlinearities will be those derived from graded-index waveguides, where a radial profile $v[(1/2)r^2]$ entails terms in J_-, J_-^2, etc. Higher-order terms require the *enveloping algebra* of Sp(2, $\mathfrak{R}$),[28] which generates all axis-symmetric aberrations.

Beyond this, Sp(2, $\mathfrak{R}$) also has two continuous representation series denoted by C_k^ϵ in Bargmann's notation, where $k = (1/2) + i\lambda$, $\lambda \in \mathfrak{R}$, and $\epsilon = 0$ or (1/2), and the exceptional series in the special interval $0 < k < 1$.[2] The continuous series was used long ago by Toller[34] and by Boyce[34] for partial wave analysis of quantum scattering amplitudes for Regge poles in the complex-k plane. In these representations the spectrum of J_0 is discrete but not lower bound, and Bessel functions of the third kind appear in the transform kernels.[18] In Ref. 13 all Sp(2, $\mathfrak{R}$) representation series are written for all eigenbasis pairs, in terms of Gauss and confluent hypergeometric functions. Which of these apply to other interesting optical models should be explored elsewhere.

APPENDIX A: D_k^+-MATRIX ELEMENTS

The D_k^+ unitary irreducible representation matrix elements $D_{n,n'}^k(\mathbf{M})$ given in Eq. (34) were written by Basu and Wolf,[13] for simplicity, in terms of a single hypergeometric function of the matrix parameters:

$$z = \frac{a^2 + b^2 + c^2 + d^2 + 2}{a^2 + b^2 + c^2 + d^2 - 2} = \frac{[(a+d) + i(b-c)][(a+d) - i(b-c)]}{[(a-d) + i(b+c)][(a-d) - i(b+c)]}.$$

The expression has the disadvantage, though, that the SO(2) subgroup (35), including the group origin, is mapped to the point at infinity, because for these elements $a^2 + b^2 + c^2 + d^2 = 2$. We can cast Eq. (34) into a form in which the hypergeometric series is developed

around zero, but at the cost of having two slightly different expressions for $n \geqslant n'$ and $n \leqslant n'$.

From the linear transformation formula for hypergeometric series (Ref. 35, Eq. 15.3.7), and within the index ranges with which we work, we invert z by

$$F\left[\begin{matrix} -n, & -n' \\ 1-2k-n-n' \end{matrix}; z\right] = \frac{(-n')_n (-z)^n}{(1-2k-n'-n)_n} \times F\left[\begin{matrix} -n, & 2k+n' \\ 1-n+n' \end{matrix}; \frac{1}{z}\right] + \{n \leftrightarrow n'\},$$

where the second summand is the same as the first, only with n and n' interchanged. We can verify that, for $n \leqslant n' \in \mathcal{Z}_0^+$, $(-n')_n$ is equal to $(-1)^n n'!/(n'-n)!$ and vanishes when $n > n'$. Therefore the second summand is zero when $n < n'$, and the first summand is zero when $n > n'$. We thus write, for $n \leqslant n'$,

$$D^k_{n,n'}\begin{bmatrix} a & b \\ c & d \end{bmatrix} = \frac{2^{2k}}{(n'-n)!}\left[\frac{n'!}{n!}\frac{\Gamma(2k+n')}{\Gamma(2k+n)}\right]^{1/2} \times \frac{[(a+d)-i(b-c)]^n[(a-d)-i(b+c)]^{n'-n}}{[(a+d)+i(b-c)]^{2k+n'}} \times F\left[\begin{matrix} -n, & 2k+n' \\ 1-n+n' \end{matrix}; \frac{[(a-d)+i(b+c)][(a-d)-i(b+c)]}{[(a+d)+i(b-c)][(a+d)-i(b-c)]}\right], \quad \text{(A1)}$$

and we write the same equation, with $\{n \leftrightarrow n'\}$, when $n \geqslant n'$. For the subgroup SO(2), we have $a-d=0=b+c$; one of the factors of Eq. (A1) thus vanishes unless $n=n'$; hence the matrix is diagonal, while the hypergeometric function is $F[\begin{smallmatrix} u, & v \\ w \end{smallmatrix}; 0] = 1$.

This yields Eq. (35) and serves to give a concrete formula for the boosted SO(2) in Eq. (59), namely,

$$D^k_{n,n'}\begin{bmatrix} \cos\theta & -e^{\zeta}\sin\theta \\ e^{-\zeta}\sin\theta & \cos\theta \end{bmatrix}\frac{i^{n'-n}}{(n'-n)!}\left[\frac{n'!}{n!}\frac{\Gamma(2k+n')}{\Gamma(2k+n)}\right]^{1/2} = \frac{(\cos\theta + i\sin\theta\cosh\zeta)^n(\sin\theta\sinh\zeta)^{n'-n}}{(\cos\theta - i\sin\theta\cosh\zeta)^{2k+n'}} \times F\left[\begin{matrix} -n, & 2k+n' \\ 1-n+n' \end{matrix}; \frac{\sin^2\theta\sinh^2\zeta}{\cos^2\theta+\sin^2\theta\cosh^2\zeta}\right], \quad \text{(A2)}$$

for $n \leqslant n'$, while in the opposite case we interchange n and n'.

ACKNOWLEDGMENTS

We are thankful for the support provided by the Dirección General de Asuntos del Personal Académico, Universidad Nacional Autónoma de México (UNAM), through grant IN104198 Optica Matemática. K. B. Wolf thanks José David Secada, Instituto de Ciencias Informáticas, Matemáticas y Físicas, Cuba, who originally brought to our attention applications of the discrete Hankel transform in acoustics. L. Vicent is Scholarship Awardee 150666 of the Consejo Nacional de Ciencia y Tecnología. The authors are grateful to Guillermo Krötzsch for graphical support of our results.

K. B. Wolf can be reached by e-mail at bwolf@fis.unam.mx.

*Permanent address, Instituto de Matemáticas, UNAM, Apartado Postal 273-3, 62210 Cuernavaca, Morelos, Mexico.

†Permanent address, Institute of Physics, Azerbaijan Academy of Sciences, H. Javid Prospekt 33, Baku 370143, Azerbaijan.

‡Also with Instituto de Matemáticas, UNAM, Apartado Postal 273-3, 62210 Cuernavaca, Morelos, Mexico.

REFERENCES

1. M. Moshinsky, T. H. Seligman, and K. B. Wolf, "Canonical transformations and the radial oscillator and Coulomb problems," J. Math. Phys. **13**, 901–907 (1972).
2. V. Bargmann, "Unitary irreducible representations of the Lorentz group," Ann. Math. **48**, 568–640 (1947).
3. N. M. Atakishiyev and K. B. Wolf, "Fractional Fourier–Kravchuk transform," J. Opt. Soc. Am. A **14**, 1467–1477 (1997).
4. M. Krawtchouk, "Sur une généralization des polinômes d'Hermite," C. R. Acad. Sci. Paris **189**, 620–622 (1929); A. Erdélyi, W. Magnus, F. Oberhettinger, and F. G. Tricomi, *Higher Transcendental Functions* (McGraw-Hill, New York, 1953), Vol. 2.
5. N. M. Atakishiyev and S. K. Suslov, "Difference analogs of the harmonic oscillator," Theor. Math. Phys. **85**, 1055–1062 (1991); N. M. Atakishiyev and K. B. Wolf, "Approximation on a finite set of points through Kravchuk functions," Rev. Mex. Fis. **40**, 366–377 (1994).
6. S. M. Candel, "An algorithm for the Fourier–Bessel transform," Comput. Phys. Commun. **23**, 343–352 (1981); S. M. Candel, "Simultaneous calculation of Fourier–Bessel transforms up to order *N*," Comput. Phys. Commun. **44**, 243–250 (1981); J. D. Secada, "Numerical evaluation of the Hankel transform," Comput. Phys. Commun. **116**, 278–294 (1999).
7. N. M. Atakishiyev, E. I. Jafarov, Sh. M. Nagiyev, and K. B. Wolf, "Meixner oscillators," Rev. Mex. Fis. **44**, 135–244 (1998).
8. W. Miller, Jr., *Symmetry and Separation of Variables* (Addison-Wesley, Reading, Mass., 1978); E. G. Kalnins, *Separation of Variables for Riemannian Spaces of Constant Curvature* (Wiley, New York, 1986).
9. R. Simon and K. B. Wolf, "The structure of paraxial optical systems," J. Opt. Soc. Am. A **17**, 342–355 (2000).
10. N. Wiener, *The Fourier Integral and Certain of Its Applications* (Cambridge U. Press, Cambridge, UK, 1933).
11. K. B. Wolf, *Integral Transforms in Science and Engineering* (Plenum, New York, 1979).
12. K. B. Wolf, "Canonical transforms. II. Complex radial transforms," J. Math. Phys. **15**, 2101–2111 (1974).
13. D. Basu and K. B. Wolf, "The unitary irreducible representations of SL(2, $\Re$) in all subgroup reductions," J. Math. Phys. **23**, 189–205 (1982).
14. S. Flügge, *Practical Quantum Mechanics* (Springer-Verlag, Berlin, 1994).
15. K. B. Wolf, "Equally-spaced energy spectra: the harmonic oscillator with a centrifugal barrier or with a centripetal well," Kinam **3**, 323–346 (1981); "Canonical transformations to phase variables in quantum oscillator systems. A group-theoretic solution," **4**, 293–332 (1982).
16. J. Ojeda-Castañeda and A. Noyola-Iglesias, "Nondiffracting wavefields in GRIN and free-space," Microwave Opt. Technol. Lett. **3**, 430–433 (1990).

17. L. D. Landau and E. Lifshitz, *Quantum Mechanics* (Addison-Wesley, Reading, Mass., 1968).
18. K. B. Wolf, "Canonical transforms. IV. Hyperbolic transforms: continuous series of SL(2, $\Re$) representations," J. Math. Phys. **21**, 680–688 (1980).
19. J. Meixner, "Orthogonale Polynomsysteme mit einer besonderen Gestalt der erzeugenden Funktion," J. London Math. Soc. **9**, 6–13 (1934).
20. V. Namias, "The fractional order Fourier transform and its application to quantum mechanics," J. Inst. Math. Appl. **25**, 241–265 (1980); V. Namias, "Fractionalization of Hankel transforms," J. Inst. Math. Appl. **26**, 187–197 (1980).
21. J.-P. Aubin, *Applied Functional Analysis* (Wiley-Interscience, New York, 1979); K. E. Atkinson, *An Introduction to Numerical Analysis* (Wiley, New York, 1989).
22. A. M. Perelomov, *Generalized Coherent States and Their Applications* (Springer-Verlag, Berlin, 1986).
23. A. O. Barut and L. Girardello, "New 'coherent' states associated with non-compact groups," Commun. Math. Phys. **21**, 41–55 (1971).
24. N. M. Atakishiyev, L. E. Vicent, and K. B. Wolf, "Continuous vs. discrete fractional Fourier transforms," J. Comput. Appl. Math. **107**, 73–95 (1999).
25. W. K. Wootters, "A Wigner-function formulation of finite-state quantum mechanics," Ann. Phys. **176**, 1–21 (1987).
26. T. Hakioğlu, "Finite-dimensional Schwinger basis, deformed symmetries, Wigner function, and an algebraic approach to quantum phase," J. Phys. A **31**, 6975–6994 (1998); "Linear canonical transformations and quantum phase: a unified canonical and algebraic approach," **32**, 4111–4130 (1999); T. Hakioğlu and E. Tepedelenlioğlu, "The action-angle Wigner function: a discrete and algebraic phase space formalism," J. Phys. A (to be published).
27. E. Wigner, "On the quantum correction for thermodynamic equilibrium," Phys. Rev. **40**, 749–759 (1932); H.-W. Lee, "Theory and application of the quantum phase-space distribution functions," Phys. Rep. **259**, 147–211 (1995); H. O. Bartelt, K.-H. Brenner, and H. Lohmann, "The Wigner distribution function and its optical production," Opt. Commun. **32**, 32–38 (1980).
28. D. D. Holm and K. B. Wolf, "Lie–Poisson description of Hamiltonian ray optics," Physica D **51**, 189–199 (1991).
29. N. M. Atakishiyev, S. M. Chumakov, and K. B. Wolf, "Wigner distribution function for finite systems," J. Math. Phys. **39**, 6247–6261 (1998).
30. S. T. Ali, N. M. Atakishiyev, S. M. Chumakov, and K. B. Wolf, "The Wigner function for general Lie groups and the wavelet transform," Ann. Inst. Henri Poincaré Phys. Theor. **1**, 685–714 (2000).
31. G. S. Agarwal, "Relation between atomic coherent-state representation, state multipoles, and generalized phase-space distributions," Phys. Rev. A **24**, 2889–2896 (1981); J. C. Várilly and J. M. Gracia-Bondía, "The Moyal representation for spin," Ann. Phys. (N.Y.) **190**, 107–148 (1989); J. P. Dowling, G. S. Agarwal, and W. P. Schleich, "Wigner distribution of a general angular-momentum state: applications to a collection of two-level atoms," Phys. Rev. A **49**, 4101–4109 (1994).
32. S. M. Chumakov, A. B. Klimov, and K. B. Wolf, "Connection between two Wigner functions for spin systems," Phys. Rev. A **61**, 034101-1–034101-3 (2000).
33. S. M. Chumakov, A. Frank, and K. B. Wolf, "Finite Kerr medium: Schrödinger cats and Wigner functions on the sphere," Phys. Rev. A **60**, 1817–1823 (1999).
34. M. Toller, "Three-dimensional Lorentz group and harmonic analysis of the scattering amplitude," Nuovo Cimento **37**, 631–657 (1965); J. F. Boyce, "Relation of the O(2, 1) partial-wave expansion to the Regge representation," J. Math. Phys. **8**, 675–684 (1967); M. Toller, "An expansion of the scattering amplitude at vanishing four-momentum transfer using the representations of the Lorentz group," Nuovo Cimento **53**, 671–715 (1968).
35. M. Abramowitz and I. Stegun, eds., *Handbook of Mathematical Functions*, Vol. 55 of Applied Mathematics Series (National Bureau of Standards, Washington, D.C., 1964).